# Chiral assembly of a pair of free base porphyrins and peroxidase-like activity of iron(III) porphyrins in four-α-helix bundle structures with dimerized two-α-helix polypeptides

**Kin-ya Tomizaki,[a] Tomonori Murata,[a] Kazuaki Kaneko,[a] Akira Miike[b] and Norikazu Nishino *[a]**

[a] *Department of Applied Chemistry, Faculty of Engineering, Kyushu Institute of Technology, Tobata, Kitakyushu 804-8550, Japan*
[b] *Diagnostics Research and Production Department, Kyowa Medex Co. Ltd., Minami-isshiki, Shizuoka, 411-0932, Japan*

***Received 12th October 1999, Accepted 28th February 2000***

A 5-(4α-bromoacetamidophenyl)-10,15,20-tritolylporphyrin was incorporated into a single-chain two-α-helix polypeptide containing 29 amino acid residues *via* the thiol side chain of a Cys residue. Two molecules of two-α-helix polypeptide connecting free base porphyrin ($H_2$-porphyrin) were strongly associated to form a four-α-helix bundle structure by hydrophobic interaction among α-helix segments and porphyrin rings in aqueous solution. The dimer formation was demonstrated by gel filtration chromatography and various spectroscopic measurements. The Soret band in the UV/vis spectrum was broadened and red-shifted in aqueous solution. In the fluorescence spectrum with excitation at the Soret band the emission at 650 nm was quenched to 40% of the intensity measured in methanol. Especially, at the Soret band was observed a strongly split circular dichroism (CD) signal, which demonstrated the chiral assembly of a pair of porphyrins in a left-handed sense. With increasing methanol content, the intensity of this split signal was decreased and finally diminished probably due to dissociation of the porphyrin moieties in the peptides. The dimerized Fe(III)-porphyrin-linked two-α-helix polypeptide was examined for biomimetic peroxidase-like activity with $H_2O_2$ or 3-chloroperbenzoic acid (MCPBA) as the oxidant. The $k_{cat}/K_M$ value for the oxidation of 3,7-dimethylamino-10-methylcarbamoylphenothiazine by the polypeptide with MCPBA was increased by 5000 times compared to that with $H_2O_2$. This fact suggests that Fe(III) porphyrin was located in the hydrophobic core and more easily accommodated an organic oxidant than does $H_2O_2$. The interior of the four-α-helix bundle structure may be further designed to mimic various haemproteins.

Haemproteins play important roles in chemical reactions such as dioxygen transportation, electron transfer, and oxidation in biological systems.[1] The active cofactor haem is utilized in a variety of functions of haemproteins. The diversity of functions is attributed to the characteristic environment surrounding the haem. The differences in axial ligand(s), imidazoles (His), thiol (Cys), and thioether (Met), to the haem result in a variety of reactivities of the corresponding haemproteins. The pairs His, Met and His, His in cytochromes *c* contribute to the electron transfer reactions. A combination of His and water has been observed in peroxidases. On the other ligand, $Cys^-$ (thiolate) coordinates to the haem in cytochrome P-450 (camphor).[1]

In the past ten years, a number of metalloporphyrin-bound polypeptides designed *de novo* have been synthesized and characterized for the investigation of ligand binding and electron transfer reaction models.[2–7] DeGrado, Dutton and co-workers designed and synthesized a multi-haem-protein model by incorporating four His residues into a disulfide-bridged two-α-helix peptide, which was further dimerized with four exogenous haems.[2] Four haems and cofacial free base ($H_2$) porphyrins were organized as a photosynthetic reaction center maquette by the same group.[3] DeGrado and co-workers designed a disulfide-bridged four-α-helix peptide which consists of a pair of antiparallel two-α-helix peptides containing a His residue to bind an exogenous haem.[4] Dutton and co-workers incorporated two His residues into an antiparallel two-α-helix peptide to accommodate two haems upon dimerization into a four-α-helix bundle structure.[5] A photoactivatable flavocytochrome model peptide was designed by incorporating an additional Cys residue using the same dimerized antiparallel two-α-helix motif.[6] Haehnel and co-workers assembled four α-helices on a cyclic peptide template and introduced two exogenous haems to mimic cytochrome *b*.[7] Benson and Mihara and co-workers designed much smaller disulfide dimerized two-α-helix peptides which formed 1 : 1 complexes with exogenous Co(III) coproporphyrin[8] and mesohaem,[9] respectively.

In addition to these haemprotein models to which haems were non-covalently introduced and sandwiched by a pair of His residues, two other approaches have been attempted so far. Four α-helix bundle polypeptides on a porphyrin template is a second design, which involves an aniline hydroxylase model by Sasaki and Kaiser,[10] and the flavin-mediated electron transfer from dihydronicotinamide to Mn(III) tetrakis(*o*-aminophenyl)-porphyrin template by Mihara *et al.*[11] The third design is based on the covalent incorporation of porphyrin derivative into the side chain of an amino acid residue in an α-helix peptide. For the covalent connection, a Lys side chain is often employed and rather short peptides were designed to characterize the environment of the porphyrin rings in detail. Therefore, different from the multi-haem systems mentioned above, Benson, Pavone and Mihara and co-workers designed merely one-α-helix peptides, which were doubled on mesohaem,[12] Fe(III) and Co(III)-deuteroporphyrins[13] or by disulfide,[14] respectively, to construct at most two-α-helix peptides in solution.

In the present study, we designed an antiparallel two-α-helix peptide (Fig. 1), which contains nine Leu to form a strong hydrophobic environment for the accommodation of the hydrophobic porphyrin ring and no His to avoid the destabilization of α-helicity. Considering the bulkiness of the synthetic porphyrin derivative, we also presumed dimer formation to

DOI: 10.1039/a908199b

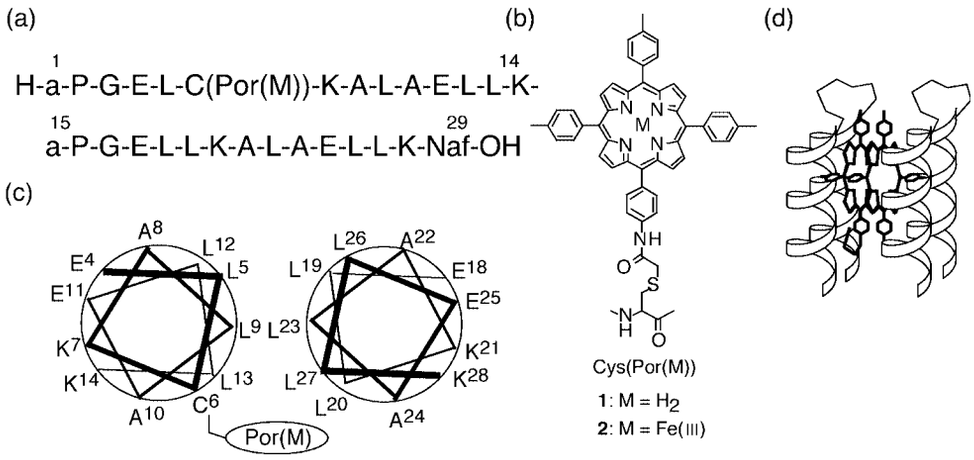


**Fig. 1** Design of porphyrin-linked two-α-helix polypeptides (M = $H_2$ (**1**) or Fe(III) (**2**)). (a) Amino acid sequence of 29-peptide, (b) porphyrin derivative attached to the thiol side chain of a Cys residue *via* a thioether linkage, (c) helical wheels of antiparallel two α-helix segments (A = Ala; a = D-Ala; C = Cys; E = Glu; G = Gly; K = Lys; L = Leu; P = Pro; Naf = L-1-naphthylalanine) and (d) possible dimer of **1** in aqueous solution.

enlarge the hydrophobic core by self-assembly of the porphyrin-linked two-α-helix peptide. In addition, we attempted to employ the thiol group of Cys for covalent linkage to the α-helix segment instead of the use of the amino group of Lys. A porphyrin derivative, 5-(4α-bromoacetamidophenyl)-10,15,20-tritolylporphyrin (Br-AcPor), was prepared and attached to the thiol side chain of the Cys residue *via* a thioether linkage.[15] This strategy avoided exposure of the porphyrin ring to anhydrous HF used for final deprotection.

Though the 29-peptide designed in the present study is equipped with no possible axial ligand, the Fe(III)-porphyrin-linked two-α-helix 29-peptide was also prepared and examined for peroxidase-like activity. The Fe(III) porphyrin placed in the hydrophobic environment was expected to behave as a primitive peroxidase before molecular evolution. The evaluation of peroxidase-like activity may help further polishing of *de novo* design by refined incorporation of appropriate ligands.

## Results and discussion

### Design and synthesis of porphyrin-linked antiparallel two-α-helix 29-peptide

The α-helix segment with eleven amino acid residues was designed by the amphiphilic α-helix motif as illustrated in Fig. 1. The hydrophobic Leu residues and two pairs of Glu and Lys residues were placed at the opposite face of the amphiphilic α-helix structure to provide hydrophobic and electrostatic interactions, respectively.[16] The α-helix segment was elongated to the N-terminal by a D-Ala-Pro-Gly sequence, which was used as an end-cap[17] and a helix-breaking loop unit when two α-helix segments were connected into the two-α-helix 29-peptide. The 29th amino acid, L-1-naphthylalanine (Naf) was introduced for synthetic convenience and as a marker during purification.[18] In order to attach the porphyrin moiety, a Cys residue was incorporated in the sixth position (first α-helix segment) which would locate at the boundary between the hydrophobic face and the hydrophilic face of the first α-helix segment. The location of the porphyrin moiety at the boundary rather than the center of the hydrophobic face might hopefully help dimerization to form a four-α-helix bundle structure with stacking of porphyrin planes[19] in the hydrophobic core.

Synthesis of the 29-peptide was carried out as previously reported.[16,20] Two pieces of protected intermediate peptides for α-helix segments were prepared by solid-phase peptide synthesis on *p*-nitrobenzophenone oxime resin using Boc chemistry and stepwise segment condensation using 1-(3-dimethylaminopropyl)-3-ethylcarbodiimide hydrochloride (EDC·HCl) and 1-hydroxybenzotriazole monohydrate (HOBt·$H_2O$) in solution (EDC–HOBt method). The side chains of Cys, Glu, and Lys residues were protected with 4-methylbenzyl (MeBzl), cyclohexyl ester (OcHex), and 2-chlorobenzyloxycarbonyl (ClZ), respectively, and the α-carboxy group of Naf was protected by benzyl ester (OBzl). The intermediate fragments were assembled convergently into two longer peptides, Boc-D-Ala-Pro-Gly-Glu(OcHex)-Leu-Cys(MeBzl)-Lys(ClZ)-Ala-Leu-Ala-Glu(OcHex)-Leu-Leu-Lys(ClZ)-OH (Boc-(1–14)-OH) and Boc-D-Ala-Pro-Gly-Glu(OcHex)-Leu-Leu-Lys(ClZ)-Ala-Leu-Ala-Glu(OcHex)-Leu-Leu-Lys(ClZ)-Naf-OBzl (Boc-(15–29)-OBzl). They were purified by gel filtration chromatography (Sephadex LH-20, 2.0 × 90 cm, dimethylformamide (DMF)) and characterized by reversed-phase high-performance liquid chromatography (RP-HPLC) and fast atom bombardment mass spectrometry (FAB-MS). Then, these two protected peptides were condensed again with the EDC–HOBt method. The obtained protected 29-peptide was successfully purified by gel filtration chromatography (Sephadex LH-60, 2.0 × 90 cm, DMF). The protecting groups were removed with anhydrous HF containing anisole for 90 min at 0 °C. The crude peptide was applied to a column of Sephadex G-50 (2.0 × 90 cm, 40% acetic acid (AcOH)) and finally purified by HPLC equipped with a YMC $C_4$ semi-preparative column (1.0 × 25 cm) eluted with a linear gradient of 37–100% $CH_3CN$/0.1% trifluoroacetic acid (TFA) over 30 min at 3 $cm^3$ $min^{-1}$ flow rate.

The Br-AcPor was prepared as reported by Lindsey *et al.*[21] It was treated with the thiol side chain of the Cys residue in the purified 29-peptide under reductive conditions containing dithiothreitol in an Ar atmosphere. To dissolve unprotected peptide and porphyrin derivative in high concentration, we found DMF containing 10% pyridine to be a favorable solvent. The desired peptide bearing $H_2$-porphyrin (**1**) was purified by gel filtration chromatography (Sephadex G-50, 2.0 × 90 cm, 40% AcOH). The $H_2$-porphyrin-linked 29-peptide, **1** was characterized by matrix assisted laser desorption ionization time-of-flight mass spectrometry (MALDI TOF-MS). The Fe(III) ion was inserted into the porphyrin planes of **1** with acetate in AcOH for 1 day at room temperature. Then, the excess of metal(II) ions was removed by gel filtration chromatography. The obtained $H_2$- and Fe(III)-porphyrin-linked two-α-helix 29-peptides (**1** and **2**) were subjected to analytical gel filtration chromatography and various spectroscopic measurements.

### Gel filtration chromatography

The two-α-helix 29-peptides, **1** and **2** were examined by gel filtration chromatography with a Superdex Peptide HR 10/30 column calibrated with the defined two marker proteins aprotinin (bovine lung, 6500) and insulin B-chain (bovine, 3496).

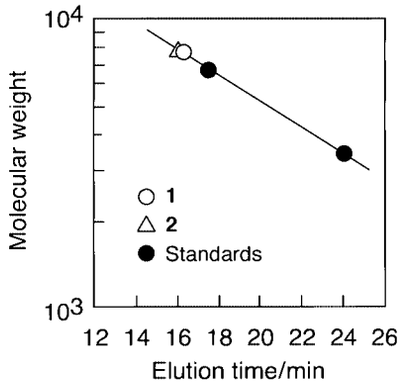


**Fig. 2** Apparent molecular mass determination of dimerized 29-peptides (**1** (open circles) and **2** (open triangles)) by gel filtration chromatography with a Superdex Peptide HR 10/30 column eluted with water detected at 420 nm at 25 °C. The column was calibrated by aprotinin (bovine lung, 6500) and insulin B-chain (bovine, 3496) (closed circles).

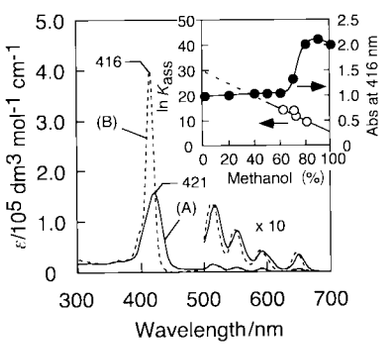


**Fig. 3** UV/vis spectra of **1** in aqueous solution (A) and in methanol (B) at 25 °C. [**1**] = $1.0 \times 10^{-5}$ mol dm$^{-3}$ (5.0 mm path length). Inset (closed circles and right axis): absorbance at 416 nm plotted as a function of methanol content. Inset (open circles and left axis): dependence of self-association constants ($K_{ass}$) for dimer of **1** on methanol content.

The apparent molecular masses in solution for **1** and **2** are shown in Fig. 2. The molecular masses obtained for the two peptides were twice their theoretical molecular weights. No peaks were observed at the elution times corresponding to the monomer and oligomers greater than the dimer. These results supported the very strong dimerization of the porphyrin-linked two-α-helix peptides to form a four-α-helix bundle structure in aqueous solution. The estimation of the association constant was carried out and described in the following section.

### UV/vis spectroscopic studies of $H_2$-porphyrin-linked two-α-helix 29-peptide

The UV/vis spectrum of **1** in aqueous solution at 25 °C exhibited the characteristic four low-energy bands (Q bands) at 650, 594, 553, 518 nm, and the broadened Soret band at 421 nm with a shoulder at 390–410 nm (Fig. 3). With increasing methanol content, all of the absorption bands in the UV/vis spectra of **1** shifted toward shorter wavelengths. Interestingly, the absorbance of the Soret band at 416 nm was significantly increased at methanol content higher than 60% (Fig. 3 (inset, right axis)). Consequently, the UV/vis spectrum of **1** in methanol exhibited Q bands at 646, 589, 549, 513 nm, and the narrow Soret band at 416 nm with a shoulder at 390–400 nm. The broadened and red-shifted Soret band of **1** at 421 nm in aqueous solution relative to that in methanol was attributed to the face-to-face association of $H_2$-porphyrin planes in a pair of the two-α-helix 29-peptides. The dimer of **1** was dissociated to the monomer by the addition of more than 70% methanol.[22] This coincided with the increase in absorbance of the narrow Soret band at 416 nm as shown in Fig. 3 (inset, right axis).

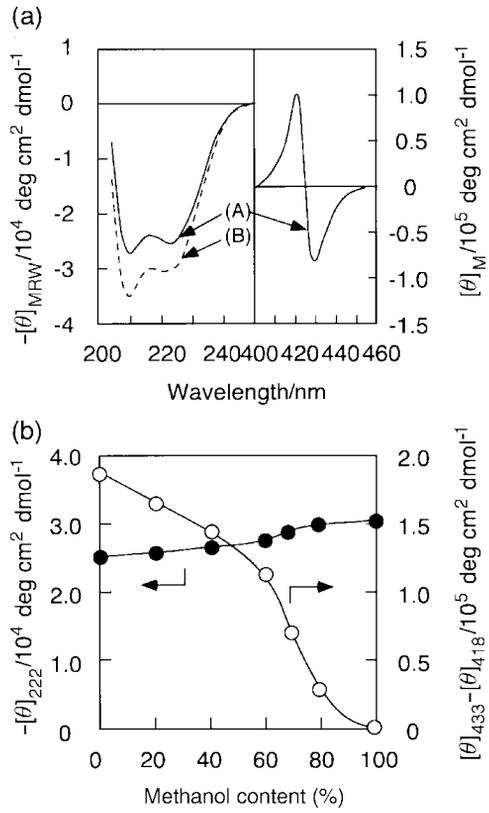


**Fig. 4** (a) CD spectra in the far-UV region and the Soret band region of **1** in aqueous solution (A) and in methanol (B) at 25 °C. (b) The ellipticity at 222 nm (closed circles) and the intensity of the split CD at Soret region ($[\theta]_{max} - [\theta]_{min}$ around 410–440 nm, open circles) plotted as a function of methanol content. [**1**] = $1.7 \times 10^{-5}$ mol dm$^{-3}$.

Since the self-association constant in water ($K_{ass}$) of **1** was too large to measure correctly, we determined the $K_{ass}$ values in aqueous solution with high methanol contents. The $K_{ass}$ values at 60–80% methanol were obtained by monitoring the decrease in absorbance at 430 nm with decreasing peptide concentration. Though a narrow range of methanol contents was explored, there appeared to be a linear relationship between the ln $K_{ass}$ values and methanol contents (Fig. 3 (inset, left axis)). By extrapolation to 0% methanol content, we roughly estimated the $K_{ass}$ value as $9.0 \times 10^{12}$ dm$^3$ mol$^{-1}$ for dimer of **1** in water. This large $K_{ass}$ value reflects the cooperative effect of the stacking of a pair of $H_2$-porphyrin planes and hydrophobic interaction of α-helix segments.

### CD studies of $H_2$-porphyrin-linked two-α-helix 29-peptide

The CD spectra of **1** in the amide region showed the typical α-helix pattern with the double minimum extrema at 222 and 208 nm in both aqueous solution and methanol (Fig. 4a). The mean residue molar ellipticities at 222 nm of **1** were −24800 deg cm$^2$ dmol$^{-1}$ in aqueous solution and −30500 deg cm$^2$ dmol$^{-1}$ in methanol, indicating the α-helicities to be 62 and 76%, respectively.[23] Therefore, in methanol, at least seven amino acid residues, probably N-terminal residues (D-Ala-Pro-Gly-), three residues (-D-Ala-Pro-Gly-) in the loop, and a C-terminal Gly residue, may be excluded from the α-helical conformation. According to Scholtz *et al.*,[24] the maximum ellipticity, −30300 deg cm$^2$ dmol$^{-1}$, was estimated with $n = 7$ in $[\theta]_{max} = (1 - n/29)40000$ deg cm$^2$ dmol$^{-1}$. Though the haem group is reported to contribute to the ellipticity in the far-UV region,[12b] the porphyrin ring connected *via* the Cys thiol group in **1** afforded almost negligible effect on the α-helicity in methanol. On the other hand, the α-helicity (62%) in aqueous solution suggested that eleven amino acid residues in the 29-peptide are not involved in α-helical conformation. This number is larger

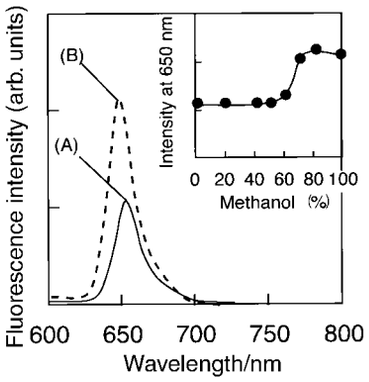


**Fig. 5** Fluorescence spectra with excitation at 420 nm of **1** in aqueous solution (A) and in methanol (B) at 25 °C. Inset: plot of the fluorescence intensity at 650 nm as a function of methanol content. [**1**] = $5.0 \times 10^{-6}$ mol dm$^{-3}$.

than expected, at most ten residues (possibly, three N-terminal residues, four residues in the loop, and three C-terminal residues) according to Scholtz *et al.*[24] The reduced α-helicity from 66% (calculated) to 62% (determined) could be the result of the destabilizing effect of the bulky $H_2$-porphyrin ring attached to the Cys residue.

We also examined the methanol content dependence of the α-helicity of **1** (Fig. 4b). At around 70% methanol the ellipticity at 222 nm of **1** changed slightly, reflecting the increase in α-helicity from 62% in aqueous solution to 76% in methanol. This fact suggests that the dissociation of the dimerized four-α-helix bundle structure of **1** in methanol was accompanied with the extension of α-helix segments in the 29-peptide.

The exciton coupled CD method is very useful for determination of the mutual orientation of chromophores.[25–27] The important interactions are between the $B_x$ and $B_y$ (π–π*) of the haem and transition dipoles of the polypeptide backbone or π–π* transition of aromatic side chains. As shown in Fig. 4a, **1** in aqueous solution showed a strongly split CD spectrum ($[\theta]_{418} - [\theta]_{433} = 1.9 \times 10^5$ deg cm$^2$ dmol$^{-1}$) consisting of negative and positive peaks, whose midpoint ($[\theta]_{424} = 0$) corresponded to the peak of the Soret band in the UV/vis spectrum (Fig. 3). Since the CD signal for the Soret band appeared negatively and positively from the longer wavelength, the transition moments in the porphyrin rings of the dimerized form of **1** may be in the left-handed orientation according to the exciton chirality principle.[26,27] The intensity of the split CD signal at the Soret band ($[\theta]_{max} - [\theta]_{min}$) of **1** decreased gradually at 0–60% methanol content and steeply at 60–80% methanol content. Finally the split CD completely disappeared in 100% methanol. The midpoint of the change in the splitting intensity appeared at 65% methanol content, where the broadened Soret band became sharp as seen in the inset of Fig. 3. The gel filtration chromatography, UV/vis, and CD spectral data were in good agreement, indicating that the $H_2$-porphyrin-linked two-α-helix 29-peptide, **1** favorably dimerized to form a four-α-helix bundle structure with association of the pair of $H_2$-porphyrins oriented in left-handed chiral position in aqueous solution.

### Fluorescence studies of $H_2$-porphyrin-linked two-α-helix 29-peptide

The fluorescence spectra of **1** with excitation at 420 nm in aqueous solution and in methanol at 25 °C are shown in Fig. 5. The fluorescence intensity in aqueous solution was quenched to 40% of that measured in methanol. The fluorescence peak in aqueous solution (652 nm) was slightly blue-shifted in methanol (649 nm). With increase in methanol content in the solution from 0 to 60% no significant change in fluorescence intensity was observed. However, at methanol contents higher than 60%, the fluorescence intensity at 650 nm of **1** was steeply increased with the midpoint at 70% methanol (Fig. 5, inset). These results support the stacking of a pair of $H_2$-porphyrins in the four-α-helix bundle structure with dimerized **1** in aqueous solution. The dissociation to the corresponding monomer around 70% methanol content was in accord with the UV/vis and CD measurements. The self-assembly of **1** depending on solution conditions was also probed by fluorescence measurements as well as by UV/vis and CD studies.

### UV/vis spectroscopic and CD studies of Fe(III)-porphyrin-linked two-α-helix 29-peptide

The UV/vis spectra of **2** was recorded in $2 \times 10^{-2}$ mol dm$^{-3}$ Tris–HCl buffer (pH 7.2) and in methanol (data not shown). The Soret band in the buffer solution of **2** appeared at 420 nm and slightly blue-shifted by 3 nm (417 nm) in methanol with an increase in absorption to 125%. Dimer formation of **2** in the buffer solution was again suggested but weakly probably due to the loss of strong stacking by insertion of Fe(III).

The CD spectra of **2** in the amide region also showed the typical α-helix pattern with the double minimum extrema at 222 and 208 nm in aqueous solution (data not shown). The mean residue molar ellipticity at 222 nm of **2** was −20000 deg cm$^2$ dmol$^{-1}$ corresponding to 50% α-helicity, which is again reduced from that of **1** (62%). The ellipticity at 222 nm of **2** was also dependent on the methanol content with the midpoint at 50% methanol which was lower than that of **1**. On the other hand, **2** showed split CD at the Soret band in aqueous solution with a negative band at 437 nm (−8000 deg cm$^2$ dmol$^{-1}$) and a positive band at 417 nm (+4000 deg cm$^2$ dmol$^{-1}$). Though the splitting intensities were smaller than those of **1** by one order of magnitude, the self-assembly of Fe(III)-porphyrins in a left-handed sense was obviously maintained with **2**.

### Oxidation of *o*-methoxyphenol by Fe(III)-porphyrin-linked two-α-helix 29-peptide

The Fe(III) porphyrin haem is a prosthetic group of haemproteins such as peroxidase and cytochrome P450.[1] Peroxidase catalyses the oxidation reaction with distal and proximal histidines.[28–31] The distal histidine may act as a general acid and base to cleave the O–O bond ionically to afford an active species (compound I) by pull effect. The proximal histidine may serve as a strong electron donor to destabilize the O–O bond by push effect. Compound I is now recognized as a Fe(IV)-oxo porphyrin π cation radical. Though the 29-peptide contains no His or other ligating group in the sequence, an examination for peroxidase-like activity seemed helpful to understand the environment where Fe(III) porphyrin was present in a four-α-helix bundle structure. The evaluation of **2** as a primitive peroxidase may also afford some clues for further evolution of artificial haemproteins.

Since *o*-methoxyphenol (guaiacol) has been employed to study peroxidase-like activity, we preliminarily subjected this reductant to **2** according to the literature[32] in combination with $H_2O_2$ as an oxidant and imidazole as axial ligands. The initial rates ($v_0$) for guaiacol oxidation catalyzed by **2** were given by measuring the increase in absorbance at 470 nm ($\varepsilon_{470} = 2.66 \times 10^4$ dm$^3$ mol$^{-1}$ cm$^{-1}$) corresponding to tetraguaiacol formation (guaiacol tetramer).[32] In the presence of an excess of guaiacol and $1.0 \times 10^{-2}$ mol dm$^{-3}$ imidazole, **2** did not oxidize the substrate at all in $2.0 \times 10^{-2}$ mol dm$^{-3}$ Tris–HCl buffer (pH 7.2) (Fig. 6). The tightly packed four-α-helix bundle structure seemed to prevent the access of substrates added in the aqueous medium to the Fe(III) porphyrin in the hydrophobic core. Previously, we introduced flavin derivatives into a single-chained four-α-helix bundle 53-peptide.[33] The flavoenzyme model showed rate enhancements in the oxidation of 1-benzyl-1,4-dihydronicotinamide in the presence of sodium *n*-hexadecanesulfonate, sodium *n*-tetradecanesulfonate, or sodium *n*-dodecanesulfonate, but not significant rate enhancements in the presence of sodium *n*-alkanesulfonates with a shorter alkyl

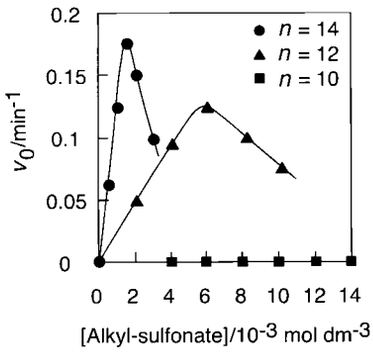


**Fig. 6** Initial rates of guaiacol oxidation catalysed by **2** depending on sodium *n*-alkanesulfonate ($C_nH_{2n+1}$-sulfonate) concentration in $2.0 \times 10^{-2}$ mol dm$^{-3}$ Tris–HCl buffer (pH 7.2) at 25 °C. [**2**] = $2.0 \times 10^{-6}$ mol dm$^{-3}$, [guaiacol] = $1.0 \times 10^{-2}$ mol dm$^{-3}$, [$H_2O_2$] = $1.0 \times 10^{-2}$ mol dm$^{-3}$, and [imidazole] = $1.0 \times 10^{-2}$ mol dm$^{-3}$.

chain length than *n*-dodecyl. The surfactant molecules were assumed to expand the tightly packed hydrophobic core of the bundle structure. Therefore, we applied a series of sodium *n*-alkanesulfonates as additives to the reaction system for peroxidase-like activity.

Interestingly, **2** showed a large rate enhancement of guaiacol oxidation in aqueous solution when sodium *n*-tetradecanesulfonate or sodium *n*-dodecanesulfonate was added to the reaction mixture. The maximum initial rates for guaiacol oxidation catalyzed by **2** were 0.175 min$^{-1}$ in the presence of $1.5 \times 10^{-3}$ mol dm$^{-3}$ sodium *n*-tetradecanesulfonate, and 0.125 min$^{-1}$ with $6.0 \times 10^{-3}$ mol dm$^{-3}$ sodium *n*-dodecanesulfonate. Further addition of these surfactants to the reaction mixture caused reduced oxidation activity of **2**. The effect of sodium *n*-tetradecanesulfonate on enhancement of guaiacol oxidation was in a narrower range than that of sodium *n*-dodecanesulfonate (Fig. 6). However, sodium *n*-decanesulfonate appeared ineffective to the catalytic activity of **2**. These results suggest that more than ten methylene groups of the surfactant and **2** may form a kind of mixed micelle as an appropriate reaction site for Fe(III) porphyrin and substrates in the four-α-helix bundle structure of **2** rather than dissociate the dimer to the corresponding monomer. Although several kinds of surfactants are known for separating the dimerized and/or oligomerized water-soluble *meso*-substituted free base porphyrins and metalloporphyrins,[34] no significant increase of absorption intensity at the Soret band in the presence of $1.5 \times 10^{-3}$ mol dm$^{-3}$ sodium *n*-tetradecanesulfonate was observed relative to that in the buffer solution (data not shown). Further addition of the surfactants caused crowding of the reactive site with alkyl chains in the mixed micelles, consequently collisions of the Fe(III) porphyrin ring, $H_2O_2$, and Fe(III) porphyrin ring and guaiacol might be disturbed.

### Oxidation of 3,7-dimethylamino-10-*N*-methylcarbamoylphenothiazine (MCDP) by Fe(III)-porphyrin-linked two-α-helix 29-peptide

Based on the observation of peroxidase-like activity examined by conventional procedures, we improved the assay method for Fe(III) porphyrin in a hydrophobic environment as follows. 3,7-Dimethylamino-10-*N*-methylcarbamoylphenothiazine (MCDP), which has been developed for clinical analysis of peroxidase activity, is a sensitive reductant producing the methylene blue molecule, which exhibits strong absorption at 666 nm ($\varepsilon_{666} = 9.6 \times 10^4$ dm$^3$ mol$^{-1}$ cm$^{-1}$).[35] Instead of $H_2O_2$, *m*-chloroperbenzoic acid (MCPBA) was employed in the oxidation of MCDP as a hydrophobic oxidant to enhance the accessibility to the Fe(III) porphyrin in the hydrophobic reaction site of **2**. An additive, $2.0 \times 10^{-5}$ mol dm$^{-3}$ *N*-α-myristoylhistidineamide (myristoyl-His-$NH_2$), was also used to represent the surfactant and imidazole in the reaction mechanism, because it seemed to be effective to expand the hydrophobic core of the bundle structure as observed in Fig. 6. Actually, the presence of myristoyl-His-$NH_2$ resulted in twice the enhancement in the initial rate for MCDP oxidation.

**Table 1** Michaelis–Menten parameters in the measurements of peroxidase-like activity of Fe(III)-porphyrin-linked 29-peptide

| Oxidant and reductant | $k_{cat}$/min$^{-1}$ | $K_M$/mol dm$^{-3}$ | $k_{cat}K_M^{-1}$/dm$^3$ mol$^{-1}$ min$^{-1}$ |
|---|---|---|---|
| MCPBA[a] | 29 | $7.5 \times 10^{-5}$ | $3.9 \times 10^5$ |
| $H_2O_2$[a] | 12 | $1.5 \times 10^{-1}$ | $8.0 \times 10^1$ |
| MCDP[b] | — | $1.3 \times 10^{-5}$ | — |

[a] [**2**] = $2.0 \times 10^{-6}$ mol dm$^{-3}$, [MCDP] = $1.0 \times 10^{-4}$ mol dm$^{-3}$, and [myristoyl-His-$NH_2$] = $2.0 \times 10^{-5}$ mol dm$^{-3}$ in $2.0 \times 10^{-2}$ mol dm$^{-3}$ Tris–HCl buffer, pH 7.2 at 25 °C. [b] [**2**] = $2.0 \times 10^{-6}$ mol dm$^{-3}$, [MCPBA] = $1.0 \times 10^{-4}$ mol dm$^{-3}$, and [myristoyl-His-$NH_2$] = $2.0 \times 10^{-5}$ mol dm$^{-3}$ in $2.0 \times 10^{-2}$ mol dm$^{-3}$ Tris–HCl buffer, pH 7.2 at 25 °C.

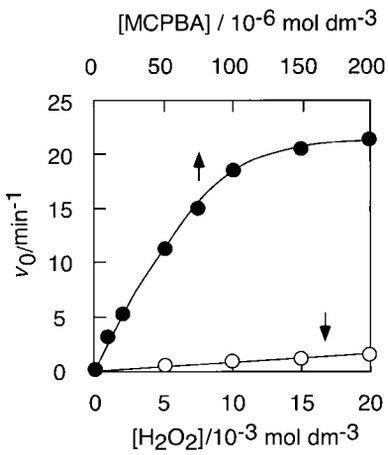


**Fig. 7** Initial rates of MCDP oxidation catalysed by **2** as functions of MCPBA (closed circles) and $H_2O_2$ (open circles) concentration in $2.0 \times 10^{-2}$ mol dm$^{-3}$ Tris–HCl buffer (pH 7.2) at 25 °C. [**2**] = $2.0 \times 10^{-6}$ mol dm$^{-3}$, [MCDP] = $1.0 \times 10^{-4}$ mol dm$^{-3}$, and [myristoyl-His-$NH_2$] = $2.0 \times 10^{-5}$ mol dm$^{-3}$.

We examined the affinity of $H_2O_2$ and MCPBA for the hydrophobic core of the dimerized four-α-helix bundle structure using MCDP as a substrate in the buffer solution (Fig. 7). Compound **2** showed saturation kinetics for MCDP oxidation as a function of MCPBA concentration between 0 and $2.0 \times 10^{-4}$ mol dm$^{-3}$, but not for MCDP oxidation with $H_2O_2$, instead linearly increasing kinetics as a function of $H_2O_2$ concentration in the range between 0 and $2.0 \times 10^{-2}$ mol dm$^{-3}$. Lineweaver–Burk plots of the $v_0$ values of MCDP oxidation against oxidant concentration gave good linear relationships. The Michaelis–Menten parameters are summarized in Table 1. The ratio ($k_{cat}/K_M$) (MCPBA) : ($k_{cat}/K_M$) ($H_2O_2$) upon MCDP oxidation was 5000 : 1. The large rate enhancement for MCDP oxidation catalyzed by **2** with MCPBA was attributed to the small $K_M$(MCPBA) value which was approximately 2000 times smaller than the $K_M(H_2O_2)$ value, indicating that MCPBA was more accessible to the hydrophobic core of the four-α-helix bundle structure than $H_2O_2$. The $k_{cat}$(MCPBA) value was 2.4 times greater than $k_{cat}(H_2O_2)$, probably due to the difference of the mechanism in activation of Fe(III) porphyrin between MCPBA and $H_2O_2$. Furthermore, MCDP was useful in detecting the peroxidase-like activity of synthetic haemprotein models because of the small $K_M$ value ($1.3 \times 10^{-5}$ mol dm$^{-3}$).

### Peroxidase-like activity of Fe(III)-porphyrin-linked two-α-helix 29-peptide under denatured conditions by methanol and guanidine hydrochloride

The four-α-helix bundle structure with dimerized porphyrin-linked 29-peptides is formed by hydrophobic interaction of

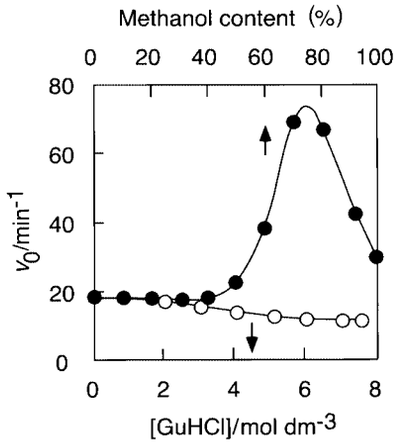


**Fig. 8** Initial rates of MCDP oxidation catalysed by **2** depending on methanol (closed circles) and GuHCl (open circles) concentration in $2.0 \times 10^{-2}$ mol dm$^{-3}$ Tris–HCl buffer (pH 7.2) at 25 °C. [**2**] = $2.0 \times 10^{-6}$ mol dm$^{-3}$, [MCDP] = $1.0 \times 10^{-4}$ mol dm$^{-3}$, [MCPBA] = $1.0 \times 10^{-4}$ mol dm$^{-3}$, and [myristoyl-His-$NH_2$] = $2.0 \times 10^{-5}$ mol dm$^{-3}$.

amphiphilic α-helix peptide segments and stacking of porphyrin rings. Such a structure loses its protein-like conformation in the presence of methanol and guanidine hydrochloride (GuHCl) in different ways. Therefore, the effects of methanol and GuHCl on the peroxidase-like activity of **2** were examined using MCDP and MCPBA as reductant and oxidant, respectively.

Fig. 8 shows the dependence of the initial rates, $v_0$ for MCDP oxidation catalyzed by **2** in the presence of $2.0 \times 10^{-5}$ mol dm$^{-3}$ myristoyl-His-$NH_2$ upon methanol content. At lower methanol contents (0–40%) no effect on the $v_0$ value was observed. With further addition of methanol to the reaction mixture the rate was enhanced and reached at 75% methanol the maximum rate (74 min$^{-1}$), which was four times greater than that in aqueous solution. At 90–100% methanol the $v_0$ values were decreased to 40% of the maximum rate obtained at 75% methanol. The tightly packed four-α-helix bundle structure of **2** might exclude the substrates from accessing its hydrophobic core in aqueous solution. The addition of the appropriate methanol content (≈75%) could modulate the bundle structure to allow access of substrates to the Fe(III) porphyrin. Since methanol contents higher than 80% dissociated the four α-helices, the loosened hydrophobic core of **2** could not accommodate substrates efficiently. On the other hand, the $v_0$ values for MCDP oxidation did not change significantly in the range of GuHCl concentration between zero and 7.5 mol dm$^{-3}$ (Fig. 8). The relative oxidation activity at 7.5 mol dm$^{-3}$ GuHCl was 65% ($v_0$ = 12.5 min$^{-1}$) based on that in aqueous solution ($v_0$ = 18.5 min$^{-1}$). At this GuHCl concentration, **2** must lose its α-helix conformation. With loss of conformation, Fe(III) porphyrin on a random coil also lost the activity enhancement at the hydrophobic reaction site on the 29-peptide.

### Comparison of Fe(III)-porphyrin-linked two-α-helix 29-peptide and horseradish peroxidase (HRP) under various conditions

The comparison of initial rates for MCDP oxidation catalyzed by **2** and HRP with MCPBA or $H_2O_2$ as oxidant is summarized in Table 2. The initial rate with $H_2O_2$ in the buffer solution of **2** was smaller than that for HRP by six orders of magnitude. Although the initial rate with MCPBA in the buffer solution of **2** was also smaller than that of HRP, the difference decreased to two orders of magnitude. The activity of **2** was enhanced by a factor of 1850 by using MCPBA as an oxidant, while that of HRP was reduced to ¼. Further, the activity of **2** in the MCDP oxidation well matched that of HRP in the buffer solution with 70% methanol. These results suggest that the peroxidase model designed *de novo* might be useful under the unusual conditions where natural enzyme could not be applied effectively.

**Table 2** Initial rates in MCDP oxidation catalysed by Fe(III)-porphyrin-linked 29-peptide and horseradish peroxidase (HRP) under various conditions

| | Initial rate of MCDP oxidation/min$^{-1}$ | | |
|---|---|---|---|
| | | MCPBA | |
| Enzyme | $H_2O_2$ in buffer | in buffer | with 70% methanol |
| **2**[a] | 0.01 | 18.5 | 70 |
| HRP[b] | 17000 | 4300 | 200 |

The initial rates were measured in $2.0 \times 10^{-2}$ mol dm$^{-3}$ Tris–HCl buffer, pH 7.2 and in the buffer solution with 70% methanol at 25 °C. Concentrations of oxidants and MCDP were fixed at $1.0 \times 10^{-4}$ mol dm$^{-3}$. [a] [**2**] = $2.0 \times 10^{-6}$ mol dm$^{-3}$ and [myristoyl-His-$NH_2$] = $2.0 \times 10^{-5}$ mol dm$^{-3}$. [b] [HRP] = $5.5 \times 10^{-8}$ mol dm$^{-3}$, determined by using $\varepsilon_{403}$ = 102000 dm$^3$ mol$^{-1}$ cm$^{-1}$ (ref. 36).

## Conclusion

We designed and synthesized porphyrin-linked two-α-helix 29-peptides which dimerized to form the four-α-helix bundle structure, burying a pair of porphyrin moieties in the hydrophobic interior in aqueous solution. The dimer formation of $H_2$-porphyrin-linked 29-peptide was promoted cooperatively by stacking of the pair of porphyrin rings and aggregation of the α-helices of two-α-helix peptides at 0–60% methanol. At higher methanol contents (60–100% methanol) the dimer was dissociated to the corresponding monomers.

We also examined peroxidase-like activity of Fe(III)-porphyrin linked 29-peptide toward guaiacol and MCDP as reductants. The hydrophobic core of the tightly packed four-α-helix bundle structure could be modulated by the addition of surfactants with more than 10 methylene groups and methanol. A hydrophobic oxidant such as MCPBA was more efficiently consumed by Fe(III)-porphyrin-linked 29-peptide. The interior made of 18 isobutyl side chains of Leu residues of the dimerized two-α-helix 29-peptides would be suitable to accommodate more hydrophobic oxidants than $H_2O_2$, the natural substrate of peroxidase.

## Experimental

### General procedures

Amino acid derivatives and reagents for peptide synthesis were purchased from Watanabe Chemical Co. (Hiroshima, Japan) and Wako Pure Chemical Industries, Ltd. (Osaka, Japan), horseradish peroxidase (type I, RZ 1.1) from Sigma. Analyses were carried out by high performance liquid chromatography (HPLC) using a Hitachi HPLC system equipped with a L-6300 Intelligent Pump, L-4200 UV-VIS Detector and D-2500 Chromato-Integrator with a Wakopak $C_4$ column (4.6 × 150 mm; 120 Å, Wako Pure Chemical Industries, Ltd.), eluted with linear gradient 37–100% $CH_3CN$–0.1% TFA over 30 min at 1 cm$^3$ min$^{-1}$ flow rate, and a Superdex Peptide HR 10/30 column (Pharmacia Biotech), eluted with water over 60 min at 0.5 cm$^3$ min$^{-1}$ flow rate. Columns of Sephadex LH-20 and LH-60 (2.0 × 90 cm, DMF) and G-50 (2.0 × 90 cm, 40% AcOH) were employed in purification. FAB-MS spectra were measured on a JEOL JMS-SX 102A mass spectrometer using Xe ionizing gas. MALDI TOF-MS was performed on a Shimadzu Kratos III mass spectrometer. $^1$H NMR spectra were measured on a JEOL JNM-A500 spectrometer.

## Syntheses

**5-(4α-Bromoacetamidophenyl)-10,15,20-tritolylporphyrin (BrAc-Por, 3).** 5-(4-Nitrophenyl)-10,15,20-tritolylporphyrin (NTTP) was prepared according to the literature.[21] To a solution of NTTP (434 mg, 0.62 mmol) in conc. HCl (100 $cm^3$) was added $SnCl_2 \cdot H_2O$ (838 mg, 3.71 mmol) and stirred for 24 h at room temperature to give 5-(4-aminophenyl)-10,15,20-tritolylporphyrin (ATTP). The reaction mixture was neutralized by 25% ammonia solution. The obtained solid was filtered off and washed with water. The crude ATTP was dissolved in $CHCl_3$, filtered, and evaporated. Yield: 400 mg (96%).

α-Bromoacetic acid (416 mg, 3.0 mmol) and dicyclohexylcarbodiimide (DCC) (309 mg, 1.5 mmol) were stirred in $CHCl_3$ (30 $cm^3$) for 30 min at 0 °C to give symmetric anhydride. To a solution of the anhydride was added ATTP (400 mg, 0.60 mmol), and stirred for 2 h at room temperature. The reaction mixture was concentrated. The organic layer was washed with water. The crude 5-(4α-bromoacetamidophenyl)-10,15,20-tritolylporphyrin (Br-AcPor) was purified by silica gel column chromatography (3.5 × 20 cm, $CHCl_3$). Yield: 428 mg (90%). FAB-MS *m*/*z* 791 and 793 $[(M)^+]$; $^1$H NMR (500 MHz, $CDCl_3$, TMS, 25 °C) $\delta$ −2.78 (s, 2H), 2.70 (s, 9H), 4.20 (s, 2H), 7.55 (d, 6H, $J$ = 7.94), 7.93 (d, 2H, $J$ = 8.24), 8.09 (d, 6H, $J$ = 7.93), 8.21 (d, 2H, $J$ = 8.24 Hz), 8.48 (s, 1H), 8.82–8.87 (m, 8H).

**Boc-D-Ala-Pro-Gly-Glu(OcHex)-Leu-Leu-Lys(ClZ)-OH (4), Boc-Ala-Leu-Ala-Glu(OcHex)-Leu-Leu-Lys(ClZ)-OPip (5), Boc-D-Ala-Pro-Gly-Glu(OcHex)-Leu-Cys(MeBzl)-Lys(ClZ)-OH (6), and Boc-Ala-Leu-Ala-Glu(OcHex)-Leu-Leu-Lys(ClZ)-Naf-OBzl (7).** Boc-D-Ala-Pro-Gly-Glu(OcHex)-Leu-Leu-Lys-(ClZ)-resin and Boc-Ala-Leu-Ala-Glu(OcHex)-Leu-Leu-Lys-(ClZ)-resin were prepared by stepwise elongation on *p*-nitrobenzophenone oxime resin using benzotriazol-1-yloxytris-(dimethylamino)phosphonium hexafluorophosphate (BOP) and 1-hydroxybenzotriazole monohydrate ($HOBt \cdot H_2O$) according to the literature.[16]

To obtain Boc-D-Ala-Pro-Gly-Glu(OcHex)-Leu-Leu-Lys(ClZ)-OH, the peptide-bound resin was shaken with *N*-hydroxypiperidine (HOPip) (4.0 equiv.) in DMF for 24 h. The reaction mixture was filtered and concentrated. The residue was dissolved in AcOH (15 $cm^3$) and sodium dithionite (5.0 equiv.) added. After 2 h stirring at room temperature, the reaction mixture was concentrated. The addition of 10% citric acid precipitated a white solid, which was filtered off, washed with water and dried. Yield of Boc-heptapeptide-OH was 80–90%. Boc-Ala-Leu-Ala-Glu(OcHex)-Leu-Leu-Lys(ClZ)-OPip was prepared without cleavage of piperidyl ester. To obtain Boc-Ala-Leu-Ala-Glu(OcHex)-Leu-Leu-Lys(ClZ)-Naf-OBzl, Boc-Ala-Leu-Ala-Glu(OcHex)-Leu-Leu-Lys(ClZ)-resin was shaken with H-Naf-OBzl tosylate (4.0 equiv.) in the presence of AcOH (4.0 equiv.) and diisopropylethylamine (DIEA) (4.0 equiv.) in DMF for 24 h. The reaction mixture was concentrated and added with 10% citric acid. The precipitated solid was filtered off and washed with water to give Boc-octapeptide-OBzl. All protected peptides were reprecipitated with methanol–diethyl ether (yield, 80–90%). The protected peptides were identified by FAB-MS: **4**, *m*/*z* 1100 $[(M + Na)^+]$, HPLC $R_t$ = 20.2 min; **5**, *m*/*z* 1191 $[(M + H)^+]$, $R_t$ = 24.0 min; **6**, *m*/*z* 1180 $[(M + Na)^+]$, $R_t$ = 21.3 min; **7**, *m*/*z* 1380 $[(M + H)^+]$, $R_t$ = 29.4 min.

**Boc-(1–14)-OH (8).** Compound **5** (476 mg, 0.40 mmol) was treated with TFA (3 $cm^3$) for 30 min at 0 °C. After concentration of the reaction mixture, the residue was precipitated with diethyl ether. The obtained H-(8–14)-OPip·TFA (90%) and **6** (431 mg, 0.36 mmol) were condensed with 1-(3-dimethylaminopropyl)-3-ethylcarbodiimide hydrochloride (EDC·HCl) (104 mg, 0.54 mmol) in the presence of $HOBt \cdot H_2O$ (67 mg, 0.43 mmol) and triethylamine ($Et_3N$) (0.05 $cm^3$, 0.36 mmol) in DMF at 0 °C for 24 h. The reaction mixture was diluted with the same volume of AcOH and then sodium dithionite (5.0 equiv.) added. The solution was stirred at room temperature for 2 h to give **8**. The crude **8** was purified by gel filtration chromatography on Sephadex LH-20 (2.0 × 90 cm, DMF). Yield: 680 mg (87%). FAB-MS *m*/*z* 2157 $[(M + Na)^+]$.

**Boc-(15–29)-OBzl (9).** Compound **4** (313 mg, 0.29 mmol) and H-(22–29)-OBzl·TFA obtained from **7** (457 mg, 0.33 mmol) were condensed in the same manner as in the preparation of **8**. The crude **9** was purified by gel filtration chromatography on Sephadex LH-20 (2.0 × 90 cm, DMF). Yield: 620 mg (91%). FAB-MS *m*/*z* 2327 $[(M + H)^+]$.

**Boc-(1–29)-OBzl (10).** Compound **8** (0.14 mmol) and H-(15–29)-OBzl·TFA (0.14 mmol) obtained from **9** were condensed in 2,2,2-trifluoroethanol (TFE) (1 $cm^3$) and dichloromethane (3 $cm^3$) using the EDC–HOBt method. The crude **10** was purified by gel filtration chromatography on Sephadex LH-60 (2.0 × 90 cm, DMF). Yield: 431 mg (70%).

**H-(1–29)-OH (11).** Compound **10** (430 mg, 0.098 mmol) was treated with anhydrous HF (10 $cm^3$) in the presence of anisole (1 $cm^3$) at 0 °C for 90 min. After removal of HF, the peptides were extracted with 10% AcOH. Then the aqueous layer was washed with diethyl ether and lyophilized to give crude **11**. This was applied to a column of Sephadex G-50 (2.0 × 90 cm, 40% AcOH) and finally purified by HPLC with a YMC $C_4$ semi-preparative column (1.0 × 25 cm) eluted with a linear gradient of 37–100% $CH_3CN$–0.1% TFA over 30 min at 3 $cm^3$ $min^{-1}$ flow rate. Yield: 200 mg, 66%. FAB-MS *m*/*z* 3102.4 $[(M + H)^+]$.

**Porphyrin attachment (1).** Compound **11** (124 mg, 0.04 mmol) and dithiothreitol (6 mg) were dissolved in DMF containing 10% pyridine (20 $cm^3$) and stirred for 1 h at 0 °C under an Ar atmosphere. To this reaction mixture was added **3** (95 mg, 0.12 mmol) in DMF solution and the mixture was stirred for 2 days under an Ar atmosphere. The solution was concentrated and applied to a Sephadex LH-60 column (2.0 × 90 cm, DMF) to remove unreacted Br-AcPor. The gel filtration chromatography was repeated four times. Then the collected fractions were evaporated and lyophilized to give **1**: 45 mg (30%). MALDI TOF-MS observed *m*/*z* 3816.8; calcd. 3812.7. GPC analysis $R_t$ = 16.30 min.

**Iron insertion (2).** To a solution of compound **1** (10 mg, 2.7 μmol) in AcOH (5 $cm^3$) was added $Fe(OAc)_2$ (200 equiv.). The reaction mixture was kept at room temperature overnight, and then concentrated. The crude peptide was purified by Sephadex G-50 gel filtration column chromatography (2.0 × 90 cm, 40% AcOH) to obtain **2**: 8.0 mg (78%). MALDI TOF-MS observed *m*/*z* 3869.6, calcd. 3866.5. GPC analysis $R_t$ = 16.05 min.

Each peptide **1** and **2** was dissolved with a small amount of TFE and stored as stock solutions.

***N*-α-Myristoyl-L-histidineamide (myristoyl-His-$NH_2$, 12).** Boc-His(Bom)-$NH_2$ (Bom, $N^{\pi}$-benzyloxymethyl, 200 mg, 0.53 mmol) was treated with TFA (2 $cm^3$) for 30 min at 0 °C. Myristic acid (145 mg, 0.63 mmol) and H-His(Bom)-$NH_2$·TFA were coupled with the EDC–HOBt method in DMF at 0 °C. Myristoyl-His(Bom)-$NH_2$ was hydrogenated on Pd–C in AcOH, and then the crude product was purified by silica gel column chromatography to give pure **12**. Yield: 104 mg (60% overall). TLC: ($CHCl_3$–methanol 9 : 1) $R_f$ 0.23. FAB-MS: *m*/*z* 365 $[(M + H)^+]$.

## Gel filtration chromatography

Gel filtration chromatography was performed on the Hitachi HPLC system described in General procedures, with the Superdex Peptide HR 10/30 column. A $3.0 \times 10^{-5}$ mol $dm^{-3}$ of sample peptide solution in water containing less than 1% TFE

was prepared. $2.5 \times 10^{-2}$ cm$^3$ of this solution was loaded. The column was calibrated by aprotinin (bovine lung, 6500) and insulin B-chain (bovine, 3496) purchased from Sigma.

### UV/vis spectroscopy

UV/vis spectra were recorded on Hitachi U-3000 and U-2010 spectrophotometers. The concentration of the **1** and **2** peptide stock solutions in methanol was determined by using $\varepsilon_{416}$ = 400900 dm$^3$ mol$^{-1}$ cm$^{-1}$ for **1** and $\varepsilon_{416}$ = 102500 dm$^3$ mol$^{-1}$ cm$^{-1}$ for **2**.

### CD measurement

CD spectra were acquired on a JASCO J-500A spectropolarimeter, routinely calibrated with (+)-camphor-10-sulfonic acid. The samples were prepared in water with various methanol contents. The typical CD spectra in the amide region were measured using 1.0 mm cuvettes at 250 to 200 nm. The Soret CD spectra were measured using 5.0 mm cuvettes in the wavelength interval 600 to 350 nm.

### Fluorescence spectroscopy

Fluorescence spectra were acquired on a Hitachi F-2500 fluorescence spectrophotometer in water containing various methanol contents at 25 °C. Spectra excited at 420 nm were measured using 1.0 cm cuvettes in the wavelength interval 525 to 775 nm.

### Kinetic measurements

Peptide **2** was dissolved in TFE as a stock solution. $H_2O_2$ (0.88 mol dm$^{-3}$) and MCPBA ($8.8 \times 10^{-3}$ mol dm$^{-3}$) (oxidants) were also dissolved in methanol as stock solutions and guaiacol (1.0 mol dm$^{-3}$) and MCDP (0.01 mol dm$^{-3}$) (marker molecules) were dissolved in methanol and DMF, respectively. A $2.0 \times 10^{-2}$ mol dm$^{-3}$ Tris–HCl buffer was transferred to a 1.0 cm quartz cuvette followed by peptide, marker molecule, and oxidant stock solutions, respectively. The final conditions were as follows: $2.0 \times 10^{-2}$ mol dm$^{-3}$ Tris–HCl buffer (pH 7.2) containing 0–100% methanol at 25 °C. The cuvette was shaken and immediately placed in the UV/vis spectrometer (Hitachi U-3000 or U-2010) to measure the absorbance at 470 nm for oxidation of guaiacol to tetraguaiacol ($\varepsilon_{470} = 2.66 \times 10^4$ dm$^3$ mol$^{-1}$ cm$^{-1}$) and at 666 nm for oxidation of MCDP to methylene blue ($\varepsilon_{666} = 9.6 \times 10^4$ dm$^3$ mol$^{-1}$ cm$^{-1}$). The increase in absorbance upon oxidation was monitored for 15 min to collect the initial rates ($v_0$). The apparent Michaelis–Menten parameters ($k_{cat}$, $K_M$, and $k_{cat}/K_M$) were obtained from at least four runs fitted with the Lineweaver–Burk equation.

## Acknowledgements

This work was partly supported by Grants-in-Aid (No. 08878087 and No. 10480153 to N. N.) from the Ministry of Education, Science and Culture, Japan.

## References

1 G. R. Moore and G. W. Pettigrew, in *Cytochromes c: Evolutionary,* Structural and Physiochemical Aspects, Springer-Verlag, Berlin, Tokyo, 1990.
2 D. E. Robertson, R. S. Farid, C. C. Moser, J. L. Urbauer, S. E. Mulholland, R. Pidikiti, J. D. Lear, A. J. Wand, W. F. DeGrado and P. L. Dutton, *Nature* (*London*), 1994, **368**, 425.
3 F. Rabanal, W. F. DeGrado and P. L. Dutton, *J. Am. Chem. Soc.*, 1996, **118**, 473.
4 C. T. Choma, J. D. Lear, M. J. Nelson, P. L. Dutton, D. E. Robertson and W. F. DeGrado, *J. Am. Chem. Soc.*, 1994, **116**, 856.
5 R. E. Sharp, J. R. Diers, D. F. Bocian and P. L. Dutton, *J. Am. Chem. Soc.*, 1998, **120**, 7103.
6 R. E. Sharp, C. C. Moser, F. Rabanal and P. L. Dutton, *Proc. Natl. Acad. Sci. U.S.A.*, 1998, **95**, 10465.
7 I. Willner, V. Heleg-Shabtai, E. Katz, H. K. Rau and W. Haehnel, *J. Am. Chem. Soc.*, 1999, **121**, 6455; H. K. Rau and W. Haehnel, *J. Am. Chem. Soc.*, 1998, **120**, 468.
8 P. A. Arnold, W. R. Shelton and D. R. Benson, *J. Am. Chem. Soc.*, 1997, **119**, 3181.
9 S. Sakamoto, S. Sakurai, A. Ueno and H. Mihara, *Chem. Commun.*, 1997, 12221.
10 T. Sasaki and E. T. Kaiser, *J. Am. Chem. Soc.*, 1989, **111**, 380.
11 H. Mihara, K. Tomizaki, T. Fujimoto, S. Sakamoto, H. Aoyagi and N. Nishino, *Chem. Lett.*, 1996, 187.
12 (*a*) P. A. Arnold, D. R. Benson, D. J. Brink, M. P. Hendrich, G. S. Jas, M. L. Kennedy, D. T. Petasis and M. Wang, *Inorg. Chem.*, 1997, **36**, 5306; (*b*) D. R. Benson, B. R. Hart, X. Zhu and M. B. Doughty, *J. Am. Chem. Soc.*, 1995, **117**, 8502.
13 F. Nastri, A. Lombardi, G. Morelli, O. Maglio, G. D'Auria, C. Pedone and V. Pavone, *Chem. Eur. J.*, 1997, **3**, 340; G. D'Auria, O. Maglio, F. Nastri, A. Lombardi, M. Mazzeo, G. Morelli, L. Paolillo, C. Pedone and V. Pavone, *Chem. Eur. J.*, 1997, **3**, 350.
14 H. Mihara, Y. Haruta, S. Sakamoto, N. Nishino and H. Aoyagi, *Chem. Lett.*, 1996, 1.
15 H. L. Levine and E. T. Kaiser, *J. Am. Chem. Soc.*, 1978, **100**, 7670.
16 H. Mihara, Y. Tanaka, T. Fujimoto and N. Nishino, *J. Chem. Soc., Perkin Trans. 2*, 1995, 1915.
17 K. R. Shoemaker, P. S. Kim, E. J. York, J. M. Stewart and R. L. Baldwin, *Nature* (*London*), 1987, **326**, 563.
18 H. Mihara, S. Lee, Y. Shimohigashi, H. Aoyagi, T. Kato, N. Izumiya and T. Costa, *Int. J. Pept. Protein Res.*, 1987, **30**, 605.
19 D. W. Urry and J. W. Pettegrew, *J. Am. Chem. Soc.*, 1967, **89**, 5276.
20 E. T. Kaiser, H. Mihara, G. A. Laforet, J. W. Kelly, L. Walters, M. A. Findeis and T. Sasaki, *Science*, 1989, **243**, 187; T. Sasaki, M. A. Findeis and E. T. Kaiser, *J. Org. Chem.*, 1991, **56**, 3159; J. C. Hendrix, K. J. Halverson and P. T. Lansbury, Jr., *J. Am. Chem. Soc.*, 1992, **114**, 7930; H. Mihara, J. A. Chmielewski and E. T. Kaiser, *J. Org. Chem.*, 1993, **58**, 2209.
21 J. S. Lindsey, I. C. Schreiman, H. C. Hsu, P. C. Kearney and A. M. Marguerettaz, *J. Org. Chem.*, 1987, **52**, 827; J. S. Lindsey and R. W. Wagner, *J. Org. Chem.*, 1989, **54**, 828.
22 G. B. Kolski and R. A. Plane, *J. Am. Chem. Soc.*, 1972, **94**, 3740.
23 Y. H. Chen, J. T. Yang and K. H. Chau, *Biochemistry*, 1974, **13**, 3350.
24 J. M. Scholtz, H. Qian, E. J. York, J. M. Stewart and R. L. Baldwin, *Biopolymers*, 1991, **31**, 1463.
25 M.-C. Hsu and R. W. Woody, *J. Am. Chem. Soc.*, 1971, **93**, 3515.
26 K. Nakanishi and N. Berova, in *Circular Dichroism-Principles and Applications*, eds. K. Nakanishi, N. Berova and R. W. Woody, VCH Publishers, Inc., New York, 1994, p. 361.
27 S. Matile, N. Berova, K. Nakanishi, J. Fleischhauer and R. W. Woody, *J. Am. Chem. Soc.*, 1996, **118**, 5198.
28 T. L. Poulos and J. Kraut, *J. Biol. Chem.*, 1980, **255**, 8199.
29 J. E. Erman, L. B. Vitello, M. A. Miller, A. Shaw, K. A. Brown and J. Kraut, *Biochemistry*, 1993, **32**, 9798.
30 S. L. Newmyer and P. R. Ortiz de Montellano, *J. Biol. Chem.*, 1995, **270**, 19430.
31 T. Matsui, S. Nagano, K. Ishimori, Y. Watanabe and I. Morishima, *Biochemistry*, 1996, **35**, 13118.
32 A. C. Maehly and B. Chance, in *Methods of Biochemical Analysis*, ed. D. Glick, John Wiley & Sons, New York, 1954, vol. 1.
33 K. Tomizaki, Y. Tsunekawa, H. Akisada, H. Mihara and N. Nishino, *J. Chem. Soc., Perkin Trans. 2*, 2000, 813; H. Mihara, K. Tomizaki, N. Nishino and T. Fujimoto, *Chem. Lett.*, 1993, 1533.
34 K. M. Kadish, G. B. Maiya, C. Araullo and R. Guilard, *Inorg. Chem.*, 1989, **28**, 2725.
35 K. Yagi, K. Kiuchi, Y. Saito, A. Miike, N. Kayahara, T. Tatano and N. Ohishi, *Biochem. Int.*, 1986, **12**, 367.
36 L. Casella, M. Gullotti, L. D. Gioia, E. Monzani and F. Chillemi, *J. Chem. Soc., Dalton Trans.*, 1991, 2945.